Biomolecules and Biomedicine
ISSN: 2831-0896 (Print) | ISSN: 2831-090X (Online)

Journal Impact Factor® (2023): 3.1
CiteScore®(2023):7.4
www.biomolbiomed.com | www.blog.bjbms.org

RESEARCH ARTICLE

Azhar et al: Adefovir's anticancer potential in HeLa cells

Adefovir anticancer potential: Network pharmacology, anti-proliferative & apoptotic effects in HeLa cells

Muzammal Mateen Azhar[1], Tahir Maqbool[1*], Fatima Ali[1], Awais Altaf[1], Muhammad Atif[2], Zulfiqar Ali[1,3], Zahid Habib Qureshi[4], Muhammad Naveed[5], Tariq Aziz[6*], Rania Ali El Hadi Mohamed[7], Fakhria A. Al-Joufi[8], Maher S. Alwethaynani[9]

[1]Centre for Research in Molecular Medicine, Institute of Molecular Biology and Biotechnology, The University of Lahore, Lahore, Pakistan;
[2]Department of Pharmacy, The University of Lahore, Lahore, Pakistan;
[3]Lahore Medical and Dental College, Lahore, Pakistan;
[4]Multan Medical and Dental College, Multan, Pakistan;
[5]Department of Biotechnology, Faculty of Science and Technology, University of Central Punjab, Pakistan;
[6]Laboratory of Animal Health Food Hygiene and Quality, University of Ioannina, Arta, Greece;
[7]Department of Biology, College of Science, Princess Nourah bint Abdulrahman University, P. O. Box 84428, Riyadh, 11671, Saudi Arabia;
[8]Department of Pharmacology, College of Pharmacy, Jouf University, 72341 Aljouf, Saudi Arabia;

[9]Department of Clinical Laboratory Sciences, College of Applied Medical Sciences, Shaqra University, Alquwayiyah, Riyadh, Saudi Arabia.

[*]Correspondence to **Tahir Maqbool**: tahir.maqbool@imbb.uol.edu.pk and **Tariq Aziz**: iwockd@gmail.com

DOI: https://doi.org/10.17305/bb.2025.12058

Guest Editor: Ziheng Wang

ABSTRACT

Cervical cancer presents a significant healthcare challenge due to recurrent disease and drug resistance, highlighting the urgent need for novel therapeutic strategies. Network pharmacology facilitates drug repurposing by elucidating multi-target mechanisms of action. Adefovir, an acyclic nucleotide analog, has shown promising potential in cervical cancer treatment, particularly in HeLa cells. *In vitro* studies have demonstrated that adefovir inhibits HeLa cell proliferation by enhancing apoptosis while maintaining a low cytotoxicity profile at therapeutic concentrations, making it an attractive candidate for further exploration. A combined network pharmacology and *in vitro* study was conducted to investigate the molecular mechanism of adefovir against cervical cancer. Potential gene targets for adefovir and cervical cancer were predicted using database analysis. Hub targets were identified, and protein-protein interaction (PPI) networks were constructed. Molecular docking assessed adefovir's binding affinity to key targets. *In vitro* cytotoxic assays, including 3-(4,5-Dimethylthiazol-2-yl)-2,5-diphenyltetrazolium bromide (MTT) and crystal violet assays, were performed using 96-well plates to evaluate anti-proliferative effects in HeLa cells. Apoptosis was assessed via p53 immunocytochemistry Enzyme-Linked Immunosorbent Assay (ELISA), while Vascular Endothelial Growth Factor ELISA (VEGF ELISA) was used to measure cell proliferation. Venn analysis identified 144 common targets between adefovir and cervical cancer. Network analysis revealed key hub targets involved in oncogenic pathways. Molecular docking demonstrated strong binding between adefovir and Mitogen-Activated Protein Kinase 3 (MAPK3) and SRC proteins. *In vitro*, adefovir significantly suppressed HeLa cell viability, with an Inhibitory Concentration 50 (IC_{50}) of 7.8 µM, outperforming 5-Fluorouracil (5-FU). Additionally, it induced apoptosis via p53 activation and inhibited cell proliferation through VEGF suppression. These integrated computational and experimental findings suggest that adefovir exerts multi-targeted effects against cervical cancer. Its promising preclinical efficacy warrants further investigation as a potential alternative therapy.

Keywords: Adefovir; HeLa cells; apoptosis; angiogenesis; network pharmacology.

INTRODUCTION

Cervical cancer's high rates of morbidity and death make it a persistent global public health concern [1]. Despite advances in surgical and chemotherapeutics interventions, treatment outcomes remain suboptimal, with high risks of recurrence of drug resistance and adverse effects posing significant challenges [2]. This underscores the urgent need for novel therapeutic strategies with improved efficacy and safety profiles. Drug repositioning offers a promising approach by identifying new clinical indications for approved drugs, thereby shortening development timelines [3]. Network pharmacology has emerged as a powerful computational framework to gain mechanistic insights into drug actions and facilitate drug repositioning opportunities [4]. It leverages omics datasets, pathways information, and systems modeling approaches to provide a holistic view of compound interactions at the molecular, pathway, and network levels [5]. Such insights can pinpoint multi-targeted mechanisms and uncover unanticipated therapeutic applications. Several network pharmacology studies have successfully identified repurposing candidates for various cancers [6].

The FDA has authorized adefovir dipivoxil, an oral bioavailable prodrug of adefovir, for the treatment of chronic hepatitis B [7]. Besides antiviral activity, recent studies have reported anti-proliferative effects of adefovir in hepatocellular carcinoma and prostate cancer [8]. However, its potential against cervical cancer remains unexplored. Given the involvement of similar oncogenic pathways like MAPK/PI3K signaling in different cancers [9], Adefovir represents an attractive candidate for network-based evaluation against cervical cancer.

The objective of this research is to examine the molecular mechanisms and therapeutic efficacy of adefovir against cervical cancer by utilizing an extensive network pharmacology experimental workflow. Integrated computational target prediction, pathway analysis, molecular docking, and experimental validation are employed to provide an in-depth understanding of adefovir's anticancer properties.

MATERIALS AND METHODS

Network pharmacology analysis

Molecular Operating Environment (MOE) 2019 (Chemical Computing Group, Montreal, Canada) was used for molecular docking. Discovery Studio Client 2021 (BIOVIA, Dassault Systèmes, San Diego, CA, USA) was employed for molecular visualization. Cytoscape v3.10.3 (Institute for

Systems Biology, Seattle, WA, USA) was utilized for hub gene identification and compound-target network generation. STRING app (Swiss Institute of Bioinformatics, Lausanne, Switzerland) was used for protein-protein interaction (PPI) network analysis. DAVID Database (Laboratory of Human Retrovirology and Immunoinformatic, Frederick, MD, USA) was applied for functional enrichment analysis. SR Plot Platform (Bioinformatics and Statistics Hub, online platform) was used to generate enrichment graphs. GraphPad Prism (GraphPad Software, Boston, MA, USA) was used for statistical analysis of *in vitro* experiments.

Adefovir-associated target prediction

Adefovir canonical SMILES were obtained from the PubChem database [10]. WAY2DRUG (DIGEP-Pred 2.0) [11] and STITCH databases [12] were analyzed to obtain the potential targets of adefovir. Adefovir's gene/target identification using Way2Drug and STITCH was based on structural similarity, pharmacophore mapping, and pathway analysis. Targets are prioritized using confidence scores (e.g., > 0.7 in STITCH). The adefovir-related target database was developed by integrating the retrieved targets and removing repetitive targets. The target names were then converted to human gene names using the UniProt databases [13].

Cervical cancer-associated target prediction

Genes linked to cervical cancer were identified by searching several open-access online databases. The databases screened included the Therapeutic Target Database, which catalogs molecular targets of drug therapies, as well as OMIM (Online Mendelian Inheritance in Man) [14] and Human Gene Databases (GeneCards) [15].

Venn analysis

A Venn diagram was generated using the bioinformatics software Venny 2.1.0 to visualize the overlap between gene sets identified in the study. Venny is a tool for comparing lists of genes/items and producing Venn diagrams [16].

Enrichment analysis of potential targets using KEGG Pathways and Gene Ontology (GO)

Gene Ontology (GO) analysis is commonly used to interpret large genomic and transcriptomic datasets. In this study, GO and pathway enrichment analysis was conducted on identified target genes to investigate their functional roles [17]. The potential target genes were organized into three

categories of gene ontology (GO) analysis based on their biological roles. GO analysis using a common online tool examined the genes involvement in biological processes, their locations within cellular components, and their molecular functions. This gene set characterization tool organized the genes into groups based on biological processes, cellular localization, and functional annotation to better understand the roles of the potential target genes. DAVID's Gene Ontology functional classification and KEGG (Kyoto Encyclopedia of Genes and Genomes) pathway mapping features were utilized. Enriched GO terms and KEGG pathways associated with the target genes with a *p*-value cutoff of 0.05 were selected for further exploration [18]. The gene ontology terms and pathways showing significant enrichment with *p*-values less than 0.05 were identified and visualized. This threshold was applied to select only the most statistically enriched results for further examination and representation. SRplot platform was used to visualize the findings in bubble chart format, demonstrating its usefulness as an online data analysis tool [19].

Protein-Protein Interactions (PPIs) and Network Analyses

Protein-protein interactions refer to the ability of proteins to bind together into complexes via non-covalent bonds between two or more protein molecules [20]. The common targets obtained through the Venn diagram were introduced into the STRING database. The STRING database was used to assess the relationship between adefovir and cervical cancer targets [21]. A protein-protein interaction network analysis was conducted to better understand how the potential target genes may interconnect at the molecular level. The analysis focused especially on human protein interactions within Homo sapiens. Cytoscape was used to generate and visualize the PPI network. Within Cytoscape, the CytoHubba plugin was employed to identify hug genes within the network based on their number of interactions (degree centrality). Higher-degree nodes that play important connectivity roles were thus highlighted. Cytoscape was also utilized to build networks linking identified drugs and targets for the purpose of examining potential therapeutic mechanisms related to cervical cancer. The network nodes were colored and shaped to distinguish drug and target genes. Edges linked interacting nodes representing protein connections [22].

Molecular docking

Structures of target proteins

The 3D structures of SRC (PDB ID: 1Y57) at a resolution 1.91 Å, ABL1 (PDB ID: 1EIP) at a resolution of 2.10 Å, PIK3CA (PDB ID: 4OVU) at a resolution of 2.96 Å, PIK3R1 (PDB ID:

1H9O) at a resolution of 1.79 Å and MAPK3 (PDB ID: 4H3Q) at a resolution of 2.2 Å were obtained in Protein Data Bank (pdb) format from the Research Collaborator for Structural Bioinformatics (RCSB) [23]. The MOE Protonate-3D module preprocessed the structure of the different proteins to ensure their docking analysis, including the removal of any co-crystallized ligands, water molecules, and other heteroatoms, as well as the addition of missing hydrogen atoms, and optimization of side-chain orientations. An AMBER99 force field was used to minimize energy and relax any steric conflicts or structural flaws in the protein structures [24].

Ligand preparation

The ligand structure was obtained from the PubChem database hosted by NCBI. Using the visualizing software Biovia Discovery Studio, the structure was converted into pdb format for further analysis. This allowed visualization and exploration of the ligands 3D structure sourced from public databases [25]. MOE first preprocessed the ligand molecule to remove counter ions and salts to generate the appropriate protonation state. The ligand was then subjected to minimize energy by using an MMFF-94x force field to obtain the most stable conformation.

Active binding site prediction of target proteins

The potential binding sites of the aimed proteins were computationally estimated. CASTp software was used to perform this analysis [26].

Molecular docking

Molecular Operating Environment (MOE version 2019.0102) was used to calculate molecular docking and scoring. The docking study was conducted for ligands against different protein targets and then visualized using the BIOVIA discovery studio visualizer. First, the ligand database is made by MOE and converted into Microsoft Access database file (MDB) format. The input files were uploaded for docking analysis with 100 ligand conformations through MOE's default docking algorithm, i.e., the Triangle Matcher, London dG, & GBVI/WSA dG for scoring functions. The best-docked result was selected after conformational visualization by BIOVIA [27].

***In vitro* anti-proliferative analysis**

HeLa cell lines

The HeLa cervical cancer cell line was provided by the Cell and Tissue Culture Laboratory at the University of Lahore. Cells are stored in cryovials in liquid nitrogen. The approval to conduct

studies was given by the "Institutional Research Ethics Committee" of the Department of Pharmacology, Faculty of Pharmacy, The University of Lahore, Pakistan.

Treatment

Adefovir (CAS number 106941-25-7) was purchased from Merck. The powdered drug was dissolved in sterile PBS to prepare 1 molar stock solution (2.73 g in 10 mL of PBS). A cell viability assay was conducted to find the optimal concentration of adefovir. Different dilutions of adefovir (1 µM, 3 µM, 5 µM, and 10 µM) were formulated in complete DMEM media from 1 M stock solution. HeLa cervical cancer cells were plated in a 96-well cell culture plate and allowed to adhere by incubating at 37 °C overnight. Growth media was removed from the wells, and the cells were rinsed with 1X PBS. Various concentrations of adefovir were introduced into the wells [28].

Study design

HeLa cells were divided into the following groups (n = 3 in each group):

1. Control: Complete DMEM medium
2. 5-FU (50 µM): 50 µM of 5-Fluorouracil in complete DMEM medium
3. Adefovir (1 µM): 1 µM of adefovir in complete DMEM medium
4. Adefovir (3 µM): 2 µM of adefovir in complete DMEM medium
5. Adefovir (5 µM): 5 µM of adefovir in complete DMEM medium
6. Adefovir (10 µM): 10 µM of adefovir in complete DMEM medium

Cell viability assay

MTT and crystal violet (CV) tests were used to measure the cell viability of treated HeLa cells. Cells were then cultivated in 96-well plates, and cell viability on various doses of the adefovir was examined.

MTT Assay

The cells were rinsed with 1X PBS and then incubated for 3-4 hours with a mixture of DMEM growth media (100 µL) and MTT reagent (25 µL). This allowed cells to metabolically reduce the MTT into insoluble purple formazan crystals. The crystals were subsequently solubilized using 10% sodium dodecyl sulfate solution. At 570 nm, absorbance was taken by a microplate reader to quantify the level of formazan present, which correlates to the number of viable cells. Cell viability percentages were derived by comparing the average absorbance values to untreated control wells [28].

CV assay

Treated cells were rinsed with 1X PBS, stained cells using 0.1% crystal violet (CV) dye solution for 15 minutes at room temperature, and then thoroughly rinsed with PBS. Care was taken during washing to avoid dislodging the stained cells from the bottom of the wells. The incorporated dye was subsequently solubilized by adding 100 µL of 1% sodium dodecyl sulfate and incubating for 5-10 minutes at room temperature. Absorbance readings at 595 nm were then obtained using a microplate reader to quantify the amount of dissolved crystal violet, which directly corresponds to the number of adherent cells [28].

Dead cells detection

For dead cell detection, a trypan blue assay was performed.

Trypan blue reagent has been used to distinguish between live and dead cells. Briefly, treated cells with adefovir were rinsed with 1X PBS and stained by trypan blue (Cat. No. T6146). The blue-stained cells were designated as dead, and they were counted using a compound microscope [28].

ELISA for *p53* and VEGF

Bioassay technology laboratory ELISA kit was used to evaluate inflammation and apoptosis. Every reagent, standard solution, and sample was made according to the instructions. Before use, all the reagents were brought to room temperature. The experiment was carried out at room temperature. The number of strips needed for the assay was established. The strips were put into the frame to use. The unused strips were stored at 2-8 °C. 50 µL standard was added to the standard well. 40 µL sample was added to the sample well, following that 10 µL at of p53 (apoptosis) and VEGF angiogenesis antibody was added to the sample. After incubating the sample and standard wells, add 50 µL of streptavidin-HRP to the sample and standard wells (excluding blank or control wells). After the mixture is thoroughly mixed, seal it with parafilm and incubate for a period of time. After the incubation, wash the well plate with wash buffer, and then add 50 µL of substrate solution A and 50 µL of substrate solution B in sequence. Incubate the well plate at 37 °C for 10 minutes. After incubation, add 50 µL of stop solution so that the blue color immediately turns to yellow. Within 10 minutes after adding the stop solution, measure the optical density at 450 nm.

Immunofluorescence with DAPI and PI

The cells were cultured on coverslips and then fixed with 4% paraformaldehyde for 15 minutes at room temperature. The cells were further permeabilized with 0.1% Triton X-100 for 10 minutes

after fixation. For nuclear staining, the cells were incubated with DAPI at a concentration of 1 µg/mL to visualize the nuclei and subsequently stained with PI at a concentration of 1 µg/mL for 10 minutes to stain dead or membrane-compromised cells. The cells were treated with PBS after staining to remove any excess dye. Fluorescence microscopy images were collected using filters for DAPI in blue and PI in red; the coverslips were mounted using a suitable mounting medium.

Ethical statement

The ethical approval for this study was granted by the Institute of Molecular Biology and Biotechnology, The University of Lahore Punjab, Pakistan.

Statistical analysis

Data from three biological replicates are presented as mean ± SD and were analyzed using one-way ANOVA followed by Tukey's multiple comparison tests. All statistical analyses were performed with GraphPad Prism 8.0 software, considering a probability value of less than 0.05 as significant. The graph indicates significance using the following abbreviations: *** for $p \leq 0.001$, ** for $p \leq 0.01$, and * for $p \leq 0.05$

RESULTS

Identification of potential targets of Adefovir and cervical cancer-related genes.

Adefovir's potential targets were predicted using the WAY2DRUG and STICH databases, identifying 182 candidate targets (Figure 2). Together with adefovir, these targets made up 183 nodes in a compound target network built with Cytoscape version 3.9.1 with 182 interactions represented as edges. Nodes for antiviral and targets were differentiated by blue and yellow color, respectively. The CytoHubba plugin of Cytoscape was used to analyze the network determining degree centrality (182), maximum neighborhood component (1), maximum clique centrality (182), closeness centrality (182), and betweenness centrality matrices (32942) for adefovir.

On the other hand, from Genecards, OMIM, and the therapeutic target database, collectively, 11,096 genes related to cervical cancer were identified. Using a Venn diagram, target genes associated with compounds, as well as those connected to cervical cancer, were submitted to identify overlapped or mutual genes. This resulted in the identification of 144 common targets (Figure 2A). Following the assumption that these targets were important, more analysis was conducted.

Interaction of protein with other proteins

To explore protein-protein interactions among potential of interest, 144 candidates were analyzed using the online database STRING version 11.5. This database generated an initial protein network linking the genes. The resulting file in TSV format was then downloaded for further analysis of the interaction data. The TSV file generated from STRING was input into Cytoscape v3.9.1 to build and visualize the protein interaction network, as shown in Figure 3B. To identify central genes, the CytoHubba degree scoring tool in cytoscape was used to rank the top 10 hub genes. SRC (55), ABL1(39), PIK3CA (37), PIK3R1(34), MAPK3(31), GRB2(31), NFkB1(29), APP (28), PTPN11(25), and SIRT1(23) have the higher degree and were processed for further analysis (Figure 3 C, D).

Pathways and GO enrichment analysis

A total of 279 important biological processes, 68 cellular constituents, 87 molecular activities, and 97 keywords related to KEGG pathways were available in the DAVID database. The target genes are mostly engaged in responding to phosphorylation, protein phosphorylation, peptidyl-tyrosine phosphorylation, and so forth, according to the biological processes (BPs). Receptor complexes, dendrites, focal adhesions, and other cellular components (CCs) are primarily engaged (Figure 3). Genes involved in transmembrane-ephrin receptor activity, protein tyrosine kinase activity, non-membrane spanning tyrosine kinase activity, and other processes were identified by molecular functions (Figure 4).

Active binding sites of target proteins

Active binding sites of the target proteins were predicted using CASTp analysis. The findings were summarized in Table 1 and Figure 5, which details the number of binding pockets, their surface areas, and the volumes of each pocket.

Molecular docking analysis

The molecular docking analysis of adefovir and 5-FU with various target proteins revealed significant differences in binding affinities and interaction characteristics. For the SRC protein, Adefovir exhibited a strong binding score of -5.5749 kJ/mol with an RMSD of 1.7828 Å, interacting primarily with residues GLU93, ARG95, TYR382, LEU410, and VAL313, while 5-FU showed a lower affinity (-4.0853 kJ/mol, RMSD 2.1366 Å) with interactions involving ARG385, ARG409, and ARG419. ABL1 demonstrated a similar trend, with adefovir scoring -

6.0613 kJ/mol (RMSD 1.2009 Å) and interacting with GLU286, GLU255, GLY254, LYS274, and LYS271, compared to 5-FU's score of -4.1592 kJ/mol (RMSD 0.7213 Å) and interactions with THR272, GLU255, LYS271, and LYS274. For PIK3CA, 5-FU had a score of -4.2951 kJ/mol (RMSD 0.8972 Å) with residues LYS640, ASN677, GLY1007, GLY1009, and SER1008, while adefovir scored -6.1912 kJ/mol (RMSD 1.1876 Å) with HIS362, GLY364, TRP564, ASN575, LYS573, LYS419, LYS379, LYS374, GLU365. PIK3R1 showed a score of -4.4766 kJ/mol (RMSD 1.3885 Å) for 5-FU with interactions involving ARG19, ARG37, LYS41, ALA46, and VAL59, whereas adefovir scored -5.5194 kJ/mol (RMSD 0.8883 Å) with ARG19, ARG37, LYS41, ALA46, VAL59. Lastly, MAPK3 showed the highest binding score of 6.2941kJ/mol (RMSD 2.2148 Å) with adefovir strongly interacting with LYS151, SER153, ASN154, ALA35, ASP167, ARG67, GLU71, and LYS54. A score of -4.3162 kJ/mol (RMSD 0.6837 Å) for 5-FU, with interactions including THR68, LYS54, ARG62, ILE56, GLU71, and ASP167.Overall, Adefovir consistently demonstrated stronger binding affinities than 5-FU across all proteins having the highest affinity for MAPK3, suggesting its potential as a more effective therapeutic candidate.

***In vitro* anti-proliferative activity of adefovir against HeLa cell line**

Adefovir exhibited cytotoxicity in a dose-dependent manner

MTT assay was performed to determine the antiproliferative activity of adefovir against human HeLa cells. HeLa cells were treated with increasing concentrations (1, 3, 5, 10 µM of adefovir for 24 h. The results show that as the concentration of the compound increases from 1 µM to 10 µM, absorbance and cell viability decrease, indicating higher doses had a greater inhibitory impact on cell proliferation with an IC_{50} value of 7.8 µM (Figure 8). CV assay was also performed to determine cell viability, indicating a more pronounced anti-proliferative effect of adefovir on HeLa cells on doses higher than 3 µM as compared to 5-FU (Figure 9)

Adefovir-induced cell death in HeLa cell line

A trypan blue assay was performed to indicate cell death caused by adefovir; Trypan blue staining revealed that over 50% of HeLa cells experienced cell death after receiving treatment with adefovir (Figure 10).

Anti-proliferation through ELISA of VEGF

The bar graph shows the effect of various treatments on VEGF concentrations. The control group showed the highest VEGF levels at 300 ng/L. Treatment with 5-FU reduced VEGF slightly to over

250 ng/L. Lower doses of the experimental drug adefovir performed similarly, with 1 μM decreasing VEGF to around 250 ng/L. Higher doses of adefovir significantly reduced VEGF in a dose-dependent manner, with 10 μM adefovir achieving the strongest inhibitory effect and lowest VEGF of approximately 50 ng/L.

Apoptosis through ELISA of p53

The bar graph depicts the concentration of p53 protein across different treatment groups. The control group exhibited the lowest levels of p53, while treatment with 50 μM 5-FU resulted in markedly higher protein concentrations. Adefovir treatment induced p53 in a dose-dependent manner, with progressively darker shades of purple representing rising concentrations from 1 to 10 μM. In particular, the 5 and 10 μM doses of adefovir significantly elevated p53 compared to the lower 1 and 3 μM doses. Overall, the data demonstrates that both 5-FU and adefovir exposure can increase p53 protein levels relative to untreated controls.

PI staining displayed the anti-proliferative potential of Adefovir

DAPI and PI staining showed marked differences in cell shape and number in control and adefovir-treated cells, indicating strong anticancer activity of adefovir as compared to 5-FU.

DISCUSSION

Cervical cancer is one of the leading causes of cancer-related deaths among females worldwide [29]. Despite advancements in treatment modalities, recurrence and development of resistance poses a serious challenge. Therefore, there is an urgent need to explore new therapeutic strategies [30]. The current study adopted a comprehensive network pharmacology approach to gain insights into the mechanism of action of Adefovir, an anti-hepatitis B virus drug, against cervical cancer.

Initially, potential targets of Adefovir and genes associated with cervical cancer were identified through databases. A total of 182 Adefovir targets and 11,096 cervical cancer genes were retrieved. Venn analysis revealed 144 common targets between adefovir and cervical cancer. The protein-protein interaction network of these 144 targets constructed using STRING was visualized by cytoscape. A large protein-protein interaction network with 149 nodes and 614 edges indicated extensive interconnectivity between targets. Highly interconnected proteins or hubs that play crucial roles in cellular processes were identified. The top 10 hubs, such as SRC, ABL1, PIK3CA, PIK3R1, and MAPK3, belong to key signaling pathways that are deregulated in cancer (Figure 3).

Pathway and gene ontology (GO) enrichment analysis provides functional insights. The significant enrichment of targets in biological processes like phosphorylation and protein modification indicated that adefovir may exert effects by modulating critical signaling mechanisms implicated in cancer [31]. The cellular component analysis found enrichment in focal adhesion and dendrites supporting a role in cytoskeleton remodeling and cell migration. Together, these in silico analyses suggested plausible anticancer mechanisms of adefovir and highlighted potential therapeutic targets.

The next crucial step was to evaluate direct binding interactions between adefovir and prioritized targets. 3D proteins structures of top 5 hub targets SRC, ABL1, PIK3CA, PIK3R1, and MAPK3 were retrieved from PDB. Active binding pockets were identified using CASTp. Molecular docking of adefovir and 5-FU (standard chemotherapeutic agent) was performed using Molecular Operating Environment (MOE). Across all targets, adefovir demonstrated consistently stronger binding affinities compared to 5-FU, with the highest scores observed for MAPK3 (Table 2). These proteins are involved in critical cancer-related pathways such as SR in the MAPK signaling pathway [32], ABL1 in JAK/STAT signaling [33], PIK3CA in the PIK3-Akt pathway [34], and MAPK3 in the Ras signaling pathway [35]. These pathways are known to play important roles in processes like proliferation, survival, angiogenesis, and metastasis when dysregulated in cancer. Binding mode analyses revealed that adefovir formed favorable interactions with key residues at the active site. These in silico docking experiments provided preliminary evidence on the capability of adefovir to directly target important cervical cancer proteins [36].

To complement computational analysis, experimental assessment was carried out using the HeLa cervical cancer cell line model. MTT, crystal violet, and trypan blue assays established that adefovir potentially inhibited HeLa cell proliferation & induced cell death in a dose-dependent manner, as performed by Rafi et al. [37] (Figure 8-12). Remarkably, adefovir showed superior anti-proliferative effects compared to 5-FU at higher concentrations. DAPI/PI staining also demonstrated morphological changes induced by adefovir treatment. Collectively, these findings validated the anticancer activity of adefovir, which was predicted by network analyses. The observed IC_{50} of 7.8 µM also suggests clinically achievable concentrations. The results from our study demonstrate that adefovir treatment significantly enhances the expression of p53 in HeLa cells as compared to the untreated control group. This observation is supported by the distinct increase in mean expression levels of p53 across the treatment groups, as measured by ELISA p53

is an important tumor suppressor protein, which is also known as the “guardian of the genome” because of its involvement in cell cycle regulation, DNA repair enhancement, and apoptosis facilitation following cellular stresses or DNA damage. In many cancer cells, including HeLa cells (which originate from cervical cancer), p53 is either mutated or functionally inactivated, allowing for unchecked cell proliferation. The reactivation or upregulation of wild-type p53 is, therefore, a promising therapeutic strategy for targeting cancer cells [38].

Our findings suggest that adefovir, a nucleotide analog primarily used as an antiviral agent, may have potential anticancer properties by modulating p53 expression. Previous research has demonstrated that nucleotide analogs can induce DNA damage, leading to the activation of p53-dependent pathways. In the context of our study, the increase in p53 expression following adefovir treatment could be indicative of its role in inducing cellular stress, which in turn activates p53. This activation may lead to cell cycle arrest or apoptosis in the HeLa cells, consistent with p53’s known mechanisms of action. Research studies directed at the use of plant extract have been utilized as a procedure to counteract the impacts of vascular endothelial growth factor (VEGF). These extracts have shown the capacity to effectively reduce the levels of VEGF, subsequently prompting the suppression of angiogenesis as demonstrated by discoveries. According to the current body of research exploration, similarity in outcomes existed. When cancerous cells were exposed to treatment with adefovir, notable reductions in VEGF levels were observed [39]. This phenomenon resulted in the inhibition of angiogenesis within the cancer cells.

Overall, this study adopted a network pharmacology approach and integrated experimental validation to explore the therapeutic potential of adefovir against cervical cancer. The key findings, mechanistic insights gained, and encouraging *in vitro* data have highlighted adefovir as a promising candidate for further investigation as an alternative or adjunct treatment option.

CONCLUSION

In conclusion, this work highlights network pharmacology as an invaluable approach for elucidating multi-targeting mechanisms and reinforcing non-oncology applications of approved drugs. The encouraging preclinical outcomes warrant further investigation of adefovir through rigorous in vivo evaluation and clinical trials. Successful validation could revolutionize cervical cancer treatment by presenting an efficacious yet safer alternative to conventional chemotherapies. Broadly, the study demonstrates how integrating systems-level analyses with experimental validations can transform drug repurposing for cancer.

ACKNOWLEDGMENTS

Authors are thankful to Princess Nourah bint Abdulrahman University Researchers Supporting Project number (PNURSP2025R890), Princess Nourah bint Abdulrahman University, Riyadh, Saudi Arabia.

Conflict of interests: Authors declare no conflict of interest.

Data availability: All the data generated in this research work has been included in this manuscript.

Submitted: 14 January 2025

Accepted: 12 March 2025

Published online: 18 March 2025

REFERENCES

1. Huang J, Deng Y, Boakye D, Tin MS, Lok V, Zhang L, et al. Global distribution, risk factors, and recent trends for cervical cancer: a worldwide country-level analysis. Gynecologic oncology. 2022;164(1):85-92. https://doi.org/10.1016/j.ygyno.2021.11.005
2. Shah K, Rawal RM. Genetic and epigenetic modulation of drug resistance in cancer: challenges and opportunities. Current Drug Metabolism. 2019 Dec 1;20(14):1114-31. https://doi.org/10.2174/1389200221666200103111539
3. Parvathaneni V, Kulkarni NS, Muth A, Gupta V. Drug repurposing: a promising tool to accelerate the drug discovery process. Drug discovery today. 2019;24(10):2076-85. https://doi.org/10.1016/j.drudis.2019.06.014
4. Dash R, Munni YA, Mitra S, Dash N, Moon IS. Network Pharmacology for Drug Repositioning in Anti-Alzheimer's Drug Development. InComputational Modeling of Drugs Against Alzheimer's Disease. New York, NY: Springer US. 2023;433-463. https://doi.org/10.1007/978-1-0716-3311-3_15
5. Agamah FE, Bayjanov JR, Niehues A, Njoku KF, Skelton M, Mazandu GK, et al. Computational approaches for network-based integrative multi-omics analysis. Frontiers in Molecular Biosciences. 2022;14;9:967205. https://doi.org/10.3389/fmolb.2022.967205
6. Kandasamy T, Sen P, Ghosh SS. Multi-targeted drug repurposing approach for breast cancer via integrated functional network analysis. Molecular informatics. 2022;41(8):2100300. https://doi.org/10.1002/minf.202100300
7. Qaqish RB, Mattes KA, Ritchie DJ. Adefovir dipivoxil: a new antiviral agent for the treatment of hepatitis B virus infection. Clinical therapeutics. 2003;25(12):3084-99. https://doi.org/10.1016/S0149-2918(03)90093-2

8. Chatterjee R, Mitra A. Insights of HBV Pathogenesis and Emerging Clinical Therapies for HBV Induced HCC Patients for a Better Prognostic Outcome. Asian Journal of Medical Sciences. 2015;6(4):1-8. http://dx.doi.org/10.3126/ajms.v6i4.11884
9. Braicu C, Buse M, Busuioc C, Drula R, Gulei D, Raduly L, et al. A comprehensive review on MAPK: a promising therapeutic target in cancer. Cancers. 2019;11(10):1618. https://doi.org/10.3390/cancers11101618
10. Rojas C, Ballabio D, Sarmiento KP, Jaramillo EP, Mendoza M, et al. ChemTastesDB: A curated database of molecular tastants. Food Chemistry: Molecular Sciences. 2022;4:100090. https://doi.org/10.1016/j.fochms.2022.100090
11. Ivanov SM, Rudik AV, Lagunin AA, Filimonov DA, Poroikov VV. DIGEP-Pred 2.0: A web application for predicting drug-induced cell signaling and gene expression changes. Molecular Informatics. 2024;43(12):e202400032. https://doi.org/10.1002/minf.202400032
12. Kuhn M, Szklarczyk D, Franceschini A, Campillos M, von Mering C, Jensen LJ, et al. STITCH 2: an interaction network database for small molecules and proteins. Nucleic acids research. 2010;1;38(suppl_1):D552-6. https://doi.org/10.1093/nar/gkp937
13. McGarvey PB, Nightingale A, Luo J, Huang H, Martin MJ, Wu C, et al. UniProt genomic mapping for deciphering functional effects of missense variants. Human mutation. 2019;40(6):694-705. https://doi.org/10.1002/humu.23738
14. Amberger JS, Bocchini CA, Schiettecatte F, Scott AF, Hamosh A. OMIM. org: Online Mendelian Inheritance in Man (OMIM®), an online catalog of human genes and genetic disorders. Nucleic acids research. 2015;43(D1):D789-98. https://doi.org/10.1093/nar/gku1205
15. Fishilevich S, Zimmerman S, Kohn A, Iny Stein T, Olender T, Kolker E, et al. Genic insights from integrated human proteomics in GeneCards. Database. 2016;2016:baw030. https://doi.org/10.1093/database/baw030
16. Yang F, Yan Y, Gu Y, Wang P, Wang M, Chen J, Du X, Wang G. Network-pharmacology-based study on the mechanism of fibrates regulating HIF-1A in the treatment of ischemic stroke. https://doi.org/10.21203/rs.3.rs-4261750/v1
17. Manzoni C, Kia DA, Vandrovcova J, Hardy J, Wood NW, Lewis PA, et al. Genome, transcriptome and proteome: the rise of omics data and their integration in biomedical sciences. Briefings in bioinformatics. 2018;19(2):286-302. https://doi.org/10.1093/bib/bbw114
18. Zhang P, Feng J, Wu X, Chu W, Zhang Y, Li P. Bioinformatics analysis of candidate genes and pathways related to hepatocellular carcinoma in China: a study based on public databases. Pathology and Oncology Research. 2021;27:588532. https://doi.org/10.3389/pore.2021.588532
19. Jokelainen O, Rintala TJ, Fortino V, Pasonen-Seppänen S, Sironen R, Nykopp TK. Differential expression analysis identifies a prognostically significant extracellular matrix–enriched gene signature in hyaluronan-positive clear cell renal cell carcinoma. Scientific Reports. 2024;14(1):10626. https://doi.org/10.1038/s41598-024-61426-3
20. Ali A, Bagchi A. An overview of protein-protein interaction. Current Chemical Biology. 2015;9(1):53-65.
21. Szklarczyk D, Gable AL, Nastou KC, Lyon D, Kirsch R, Pyysalo S, et al. The STRING database in 2021: customizable protein–protein networks, and functional characterization of user-uploaded gene/measurement sets. Nucleic acids research. 2021;49(D1):D605-12. https://doi.org/10.1093/nar/gkaa1074
22. Yang X, Man D, Zhao P, Li X. Identification of the therapeutic mechanism of the saffron crocus on glioma through network pharmacology and bioinformatics analysis. Medical Oncology. 2023;40(10):296. https://doi.org/10.1007/s12032-023-02142-2

23. Burley SK, Bhikadiya C, Bi C, Bittrich S, Chao H, Chen L, et al. RCSB Protein Data Bank (RCSB. org): delivery of experimentally-determined PDB structures alongside one million computed structure models of proteins from artificial intelligence/machine learning. Nucleic acids research. 2023;51(D1):D488-508. https://doi.org/10.1093/nar/gkac1077
24. Kalinowsky L, Weber J, Balasupramaniam S, Baumann K, Proschak E. A diverse benchmark based on 3D matched molecular pairs for validating scoring functions. ACS omega. 2018;3(5):5704-14. https://doi.org/10.1021/acsomega.7b01194
25. Gupta A, Sahu N, Singh AP, Singh VK, Singh SC, Upadhye VJ, et al. Exploration of novel lichen compounds as inhibitors of SARS-CoV-2 Mpro: ligand-based design, molecular dynamics, and ADMET analyses. Applied Biochemistry and Biotechnology. 2022;194(12):6386-406. https://doi.org/10.1007/s12010-022-04103-3.
26. Tian W, Chen C, Lei X, Zhao J, Liang J. CASTp 3.0: computed atlas of surface topography of proteins. Nucleic acids research. 2018;46(W1):W363-7. https://doi.org/10.1093/nar/gky473
27. Seyedhosseini Ghaheh H, Damavandi MS, Sadeghi P, Massah AR, Asl TH, Salari-Jazi A, et al. Targeting and ultrabroad insight into molecular basis of resistance-nodulation-cell division efflux pumps. Scientific Reports. 2022;12(1):16130. https://doi.org/10.1038/s41598-022-20278-5
28. Maqbool T, Awan SJ, Malik S, Hadi F, Shehzadi S, Tariq K. In-vitro anti-proliferative, apoptotic and antioxidative activities of medicinal herb Kalonji (Nigella sativa). Current pharmaceutical biotechnology. 2019;20(15):1288-308. https://doi.org/10.2174/1389201020666190821144633
29. Reza S, Dewan SM, Islam MS, Shahriar M. Response of Bangladesh to the World Health Organization call to eliminate cervical cancer as a public health issue: An observational report. Health Science Reports. 2024;7(6):e2178. https://doi.org/10.1002/hsr2.2178
30. Desai VM, Kumbhar P, Kadam AY, Swarup J, Priya S, Jain A, et al. Exploring the therapeutic modalities of targeted treatment approach for skin carcinoma: cutting-edge strategies and key insights. Expert Opinion on Drug Delivery. 2024;21(8):1213-33. https://doi.org/10.1080/17425247.2024.2392799

31. Ci M, Zhao G, Li C, Liu R, Hu X, Pan J, et al. OTUD4 promotes the progression of glioblastoma by deubiquitinating CDK1 and activating the MAPK signaling pathway. Cell Death & Disease. 2024;15(3):179. https://doi.org/10.1038/s41419-024-06569-x
32. Zhou L, Ni C, Liao R, Tang X, Yi T, Ran M, et al. Activating SRC/MAPK signaling via the 5-HT1A receptor contributes to the effect of vilazodone on improving thrombocytopenia. Elife. 2024;13:RP94765. https://doi.org/10.7554/eLife.94765.
33. Vadeikienė R, Jakštys B, Laukaitienė D, Šatkauskas S, Juozaitytė E, Ugenskienė R. The Role of Mutated Calreticulin in the Pathogenesis of BCR-ABL1-Negative Myeloproliferative Neoplasms. International journal of molecular sciences. 2024;25(18):9873. https://doi.org/10.3390/ijms25189873
34. Sutera P, Kim J, Kumar R, Deek RA, Stephenson R, Mayer T, et al. PIK3/Akt/mTOR pathway alterations in metastatic castration-sensitive prostate cancer. The Prostate. 2024;84(14):1301-8. https://doi.org/10.1002/pros.24765
35. Morgos DT, Stefani C, Miricescu D, Greabu M, Stanciu S, Nica S, et al. Targeting PI3K/AKT/mTOR and MAPK signaling pathways in gastric cancer. International Journal of Molecular Sciences. 2024;25(3):1848. https://doi.org/10.3390/ijms25031848

36. García-Trejo JJ, Ortega R, Zarco-Zavala M. Putative repurposing of lamivudine, a nucleoside/nucleotide analogue and antiretroviral to improve the outcome of cancer and COVID-19 patients. Frontiers in Oncology. 2021;11:664794. https://doi.org/10.3389/fonc.2021.664794

37. Rafi S, Maqbool T, Sarwar M, Qureshi ZH, Nasreen M, Naz S, et al. Hepatoprotective potential of lamivudine through activation of gamma-glutamyltransferase and down-regulation of p53 in HepG2 cells. https://doi.org/10.62877/136-IJCBS-24-25-19-136.

38. Ahmad I, Maqbool T, Naz S, Hadi F, Atif M. Apoptotic potential of geranyl acetate in HepG2 liver cancer cells. International Journal of Applied and Experimental Biology. 2023;2(2):89-96. https://doi.org/10.56612/ijaeb.v1i1.57

39. Hadi F, Maqbool T, Khurshid S, Nawaz A, Aftab S, Tahir S, Awan SJ, Malik A. Anti-Fungal Activity of *Cressa cretica*, *Leptadenia pyrotechnica* and *Pulicaria crispa*, Indigenous Plants of Cholistan Desert, Pakistan. Anti-Infective Agents. 2021;19(3):325-32. https://doi.org/10.2174/2211352518999201117144613

TABLES AND FIGURES WITH LEGENDS

Table 1. Binding pockets, area, volume, color, and style of the top pocket of all proteins.

Sr no	Protein	Protein (PDB)	Binding pockets	Area(SA)	Volume(SA)	Negative volume color	Representation style
1	SRC	1Y57	58	2217.453	3266.202	Red	Cartoon
2	ABL1	1IEP	64	1096.316	852.391	Red	Cartoon
3	PIK3CA	40VU	197	8023.264	7885.856	Red	Cartoon
4	PIK3R1	1H9O	14	67.140	29.788	Red	Cartoon
5	MAPK3	4H3Q	59	579.051	419.707	Red	Cartoon

Table 2. Molecular docking analysis of adefovir and 5-FU with different proteins

Proteins	Compounds	S score (kJ/mol)	RMSD (Å)	Interacting residues
SRC	Adefovir	-5.5749	1.7828	GLU93,ARG95,TYR382,LEU410,VAL313
	5FU	-4.0853	2.1366	ARG385,ARG409,ARG419
ABL1	Adefovir	-6.0613	1.2009	GLU286,GLU255,GLY254,LYS274,LYS271
	5FU	-4.1592	0.7213	THR272,GLU255,LYS271,LYS274
PIK3CA	Adefovir	-6.1912	1.1876	HIS362,GLY364,TRP564,ASN575,LYS573,LYS419, LYS379,LYS374,GLU365
	5FU	-4.2951	0.8972	LYS640,ASN677,GLY1007,GLY1009,SER1008
PIK3R1	Adefovir	-5.5194	0.8883	SER39,SER40,ARG19,ARG37
	5FU	-4.4766	1.3885	ARG19,ARG37,LYS41,ALA46,VAL59

MAPK3	Adefovir	-6.2941	2.2148	LYS151,SER153,ASN154,ALA35,ASP167,ARG67, GLU71, LYS54
	5FU	-4.3162	0.6837	THR68,LYS54,ARG67,ILE56,GLU71,ASP167

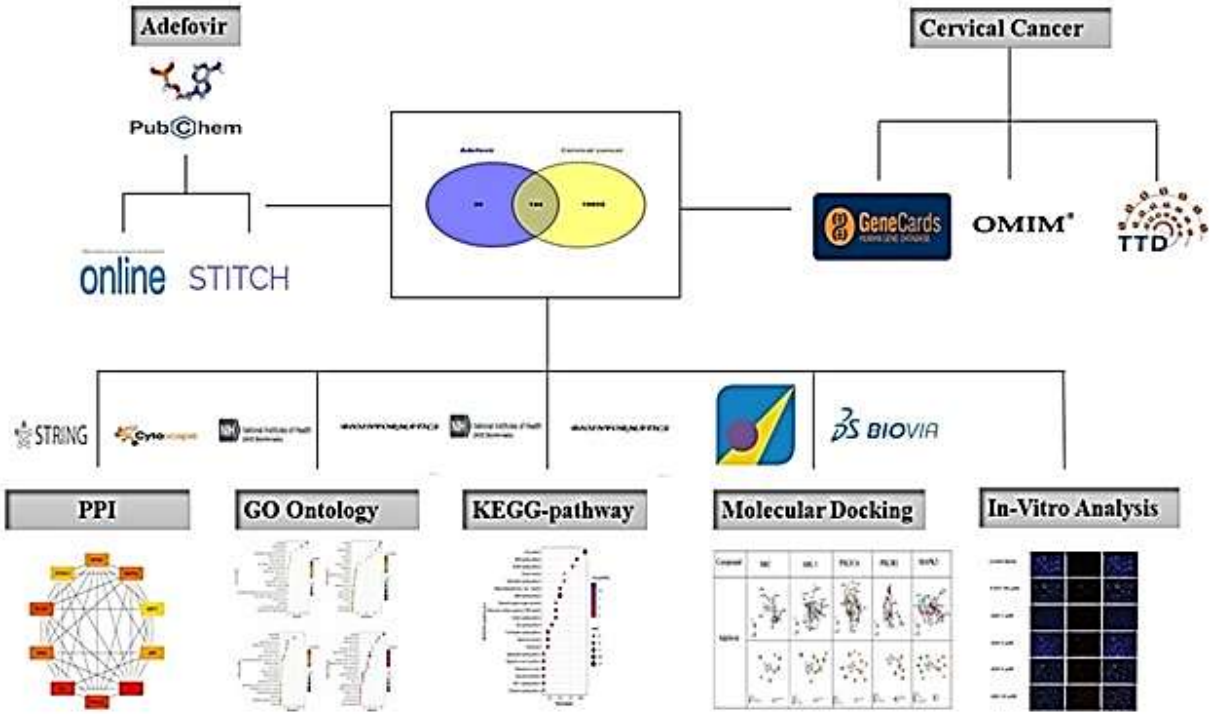

Figure 1. Graphical illustration of the study's workflow.

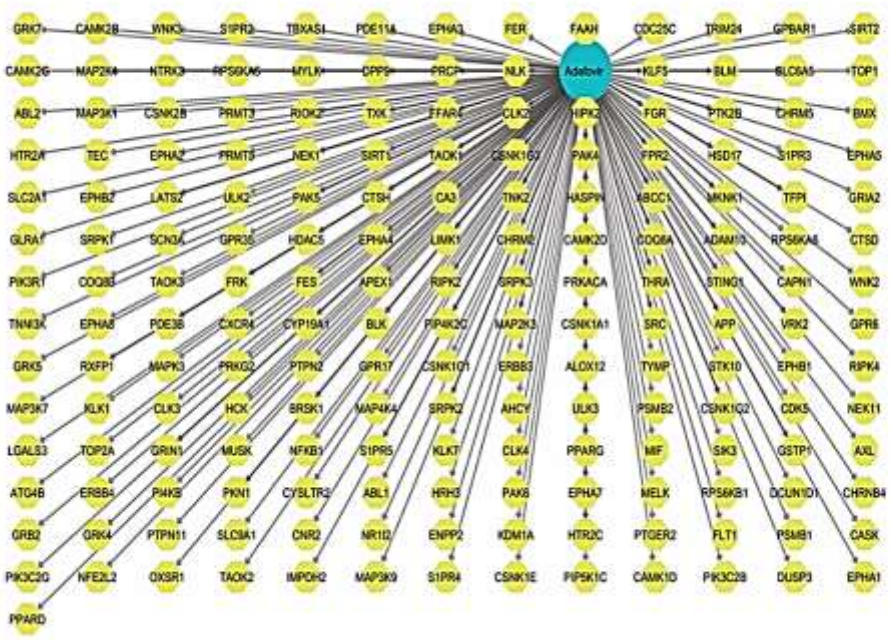

Figure 2. Adefovir's compound target network consists of 182 targets. The color blue represents the active component, while the possible targets are represented by the color yellow.

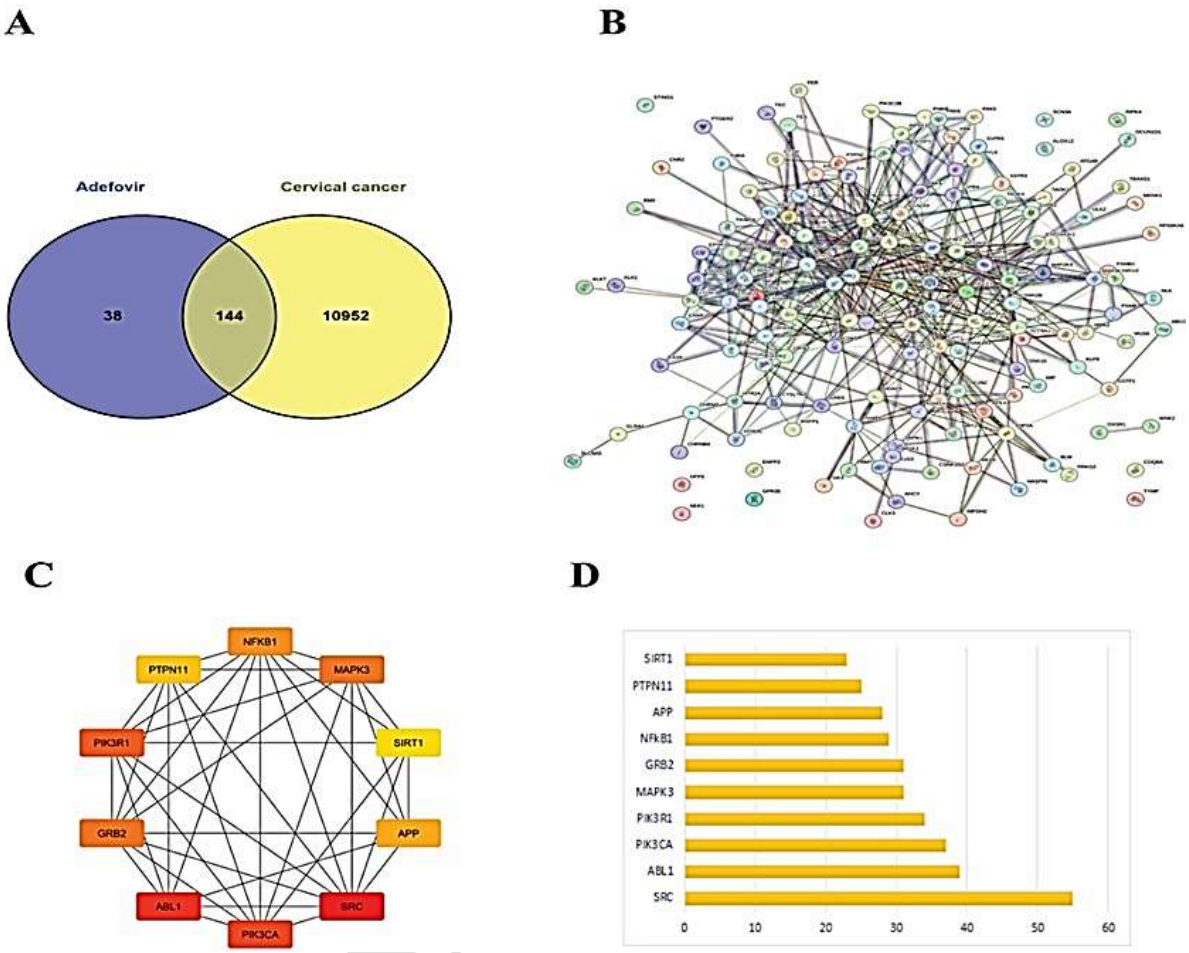

Figure 3. (A) Venn diagram showing overlapping 144 targets of adefovir out of a total 182 targets. (B) Protein-protein interaction network (PPI) of interlinking proteins (C) Top 10 hub genes (D) Scoring of top 10 hub genes.

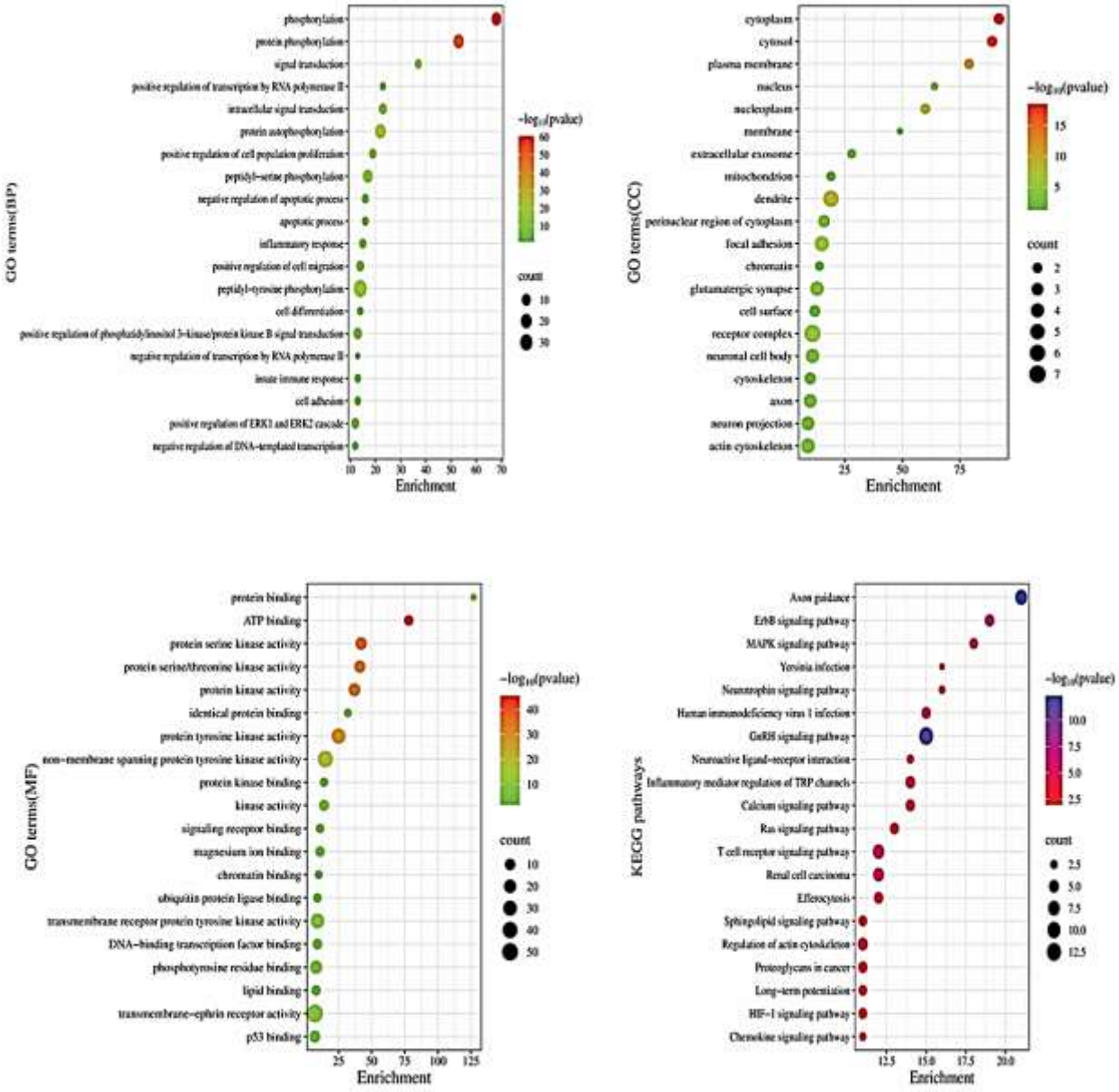

Figure 4. Shows the top 20 KEGG pathways and GO enriched terms (BP, CC, and MF), respectively.

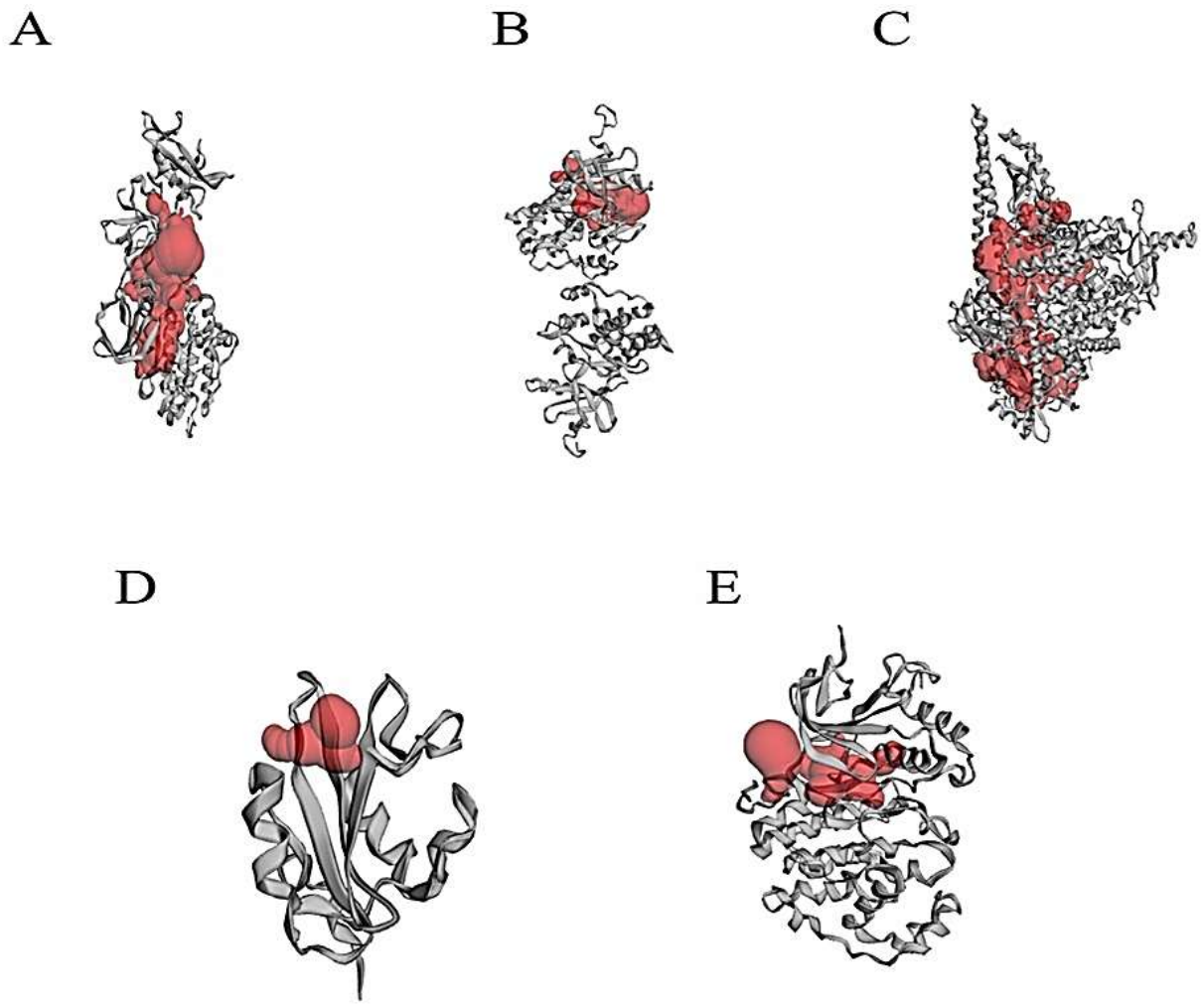

Figure 5. The active site of target proteins was obtained from the CASTp server. (A) SRC (B) ABL1 (C) PIK3CA (D) PIK3R1 (E) MAPK3

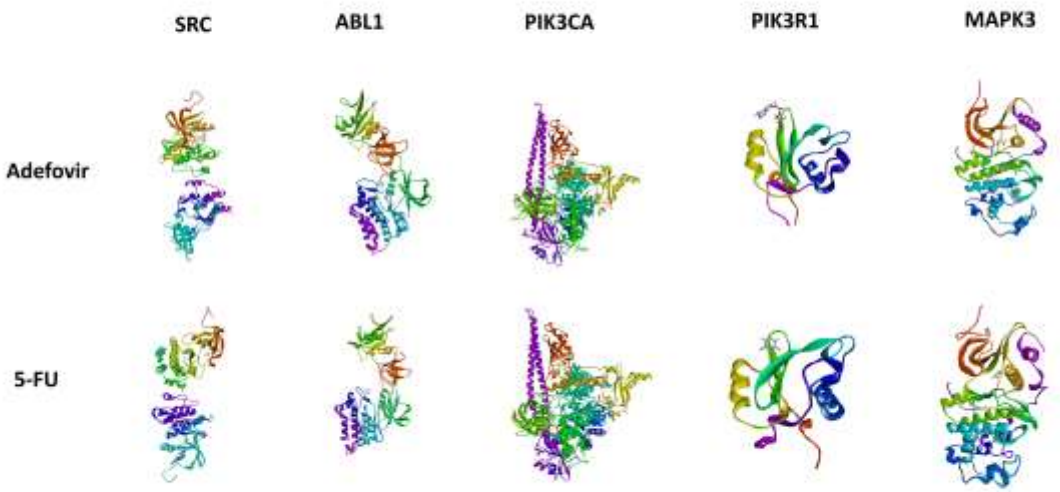

Figure 6. 3-dimensional configuration and compound interactions with different proteins.

Adefovir-SRC complex

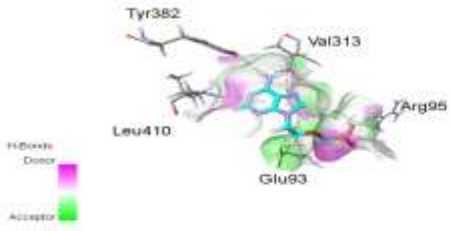

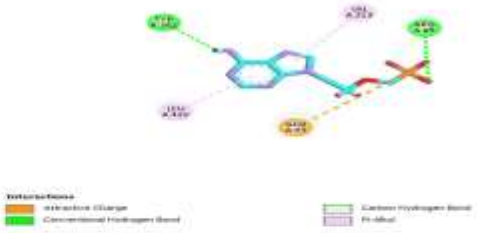

Adefovir-ABL1 complex

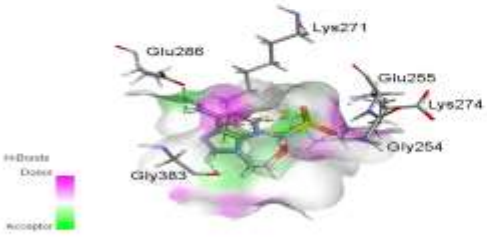

Adefovir-PIK3CA complex

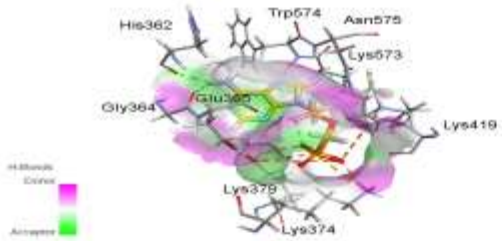

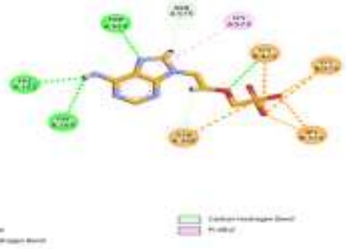

Adefovir-PIK3R1 complex

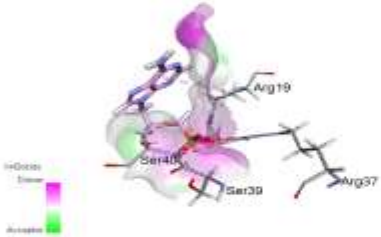

Adefovir-MAPK3 complex

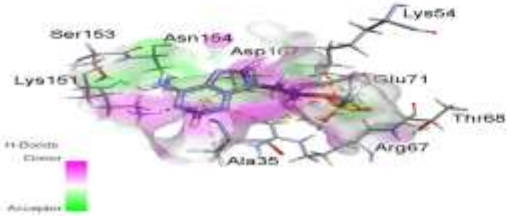

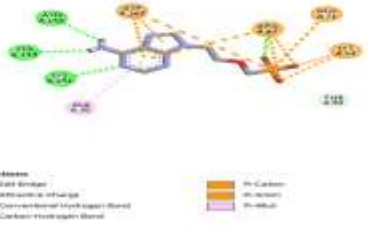

Figure 7. 2D and 3D interactions of adefovir with different cervical cancer proteins. Where molecular interactions between Adefovir and various protein complexes, including SRC, ABL1, PIK3CA, PIK3R1, and MAPK3 (detail in results). For each complex, specific amino acid residues involved in the interaction are highlighted, such as Tyr382, Val313, Leu410, and Glu93 in the SRC complex, and Glu286, Gly284, and Gly283 in the ABL1 complex.

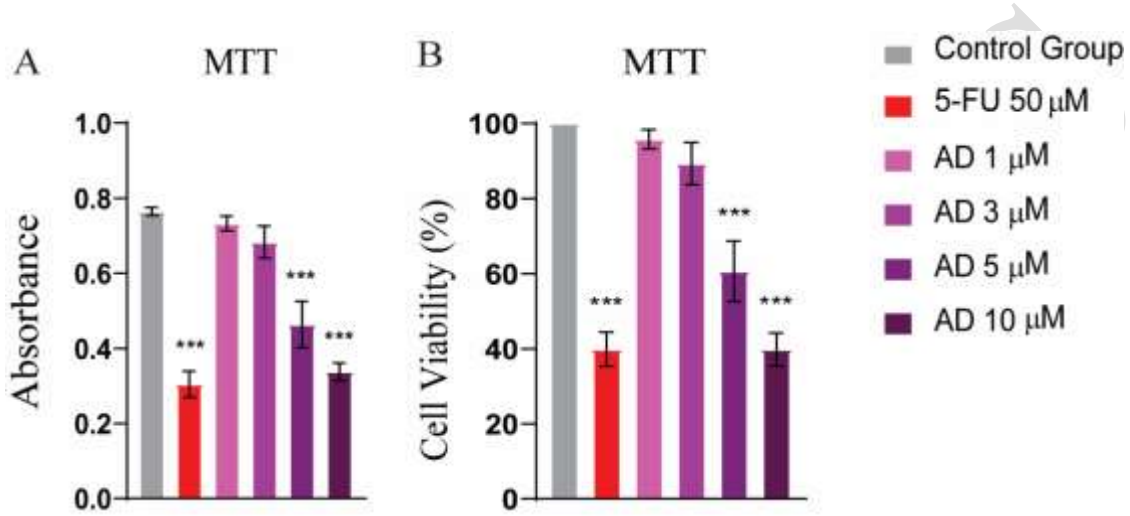

Figure 8. MTT assay showed strong anticancer potential of adefovir at doses of 5 and 10 µM. One-way ANOVA followed by Tukey's multiple comparison test, n = 3, *** ≤ 0.001.

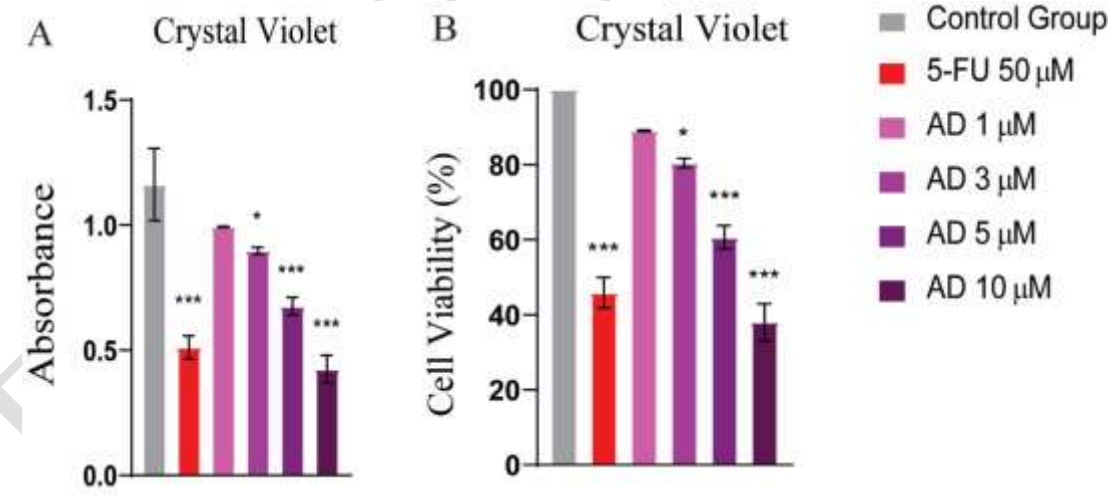

Figure 9. CV assay revealed significant anti-proliferative activity of adefovir at doses greater than 3 µM. Tukey's multiple comparison test after a one-way ANOVA, n = 3, *** ≤ 0.001.

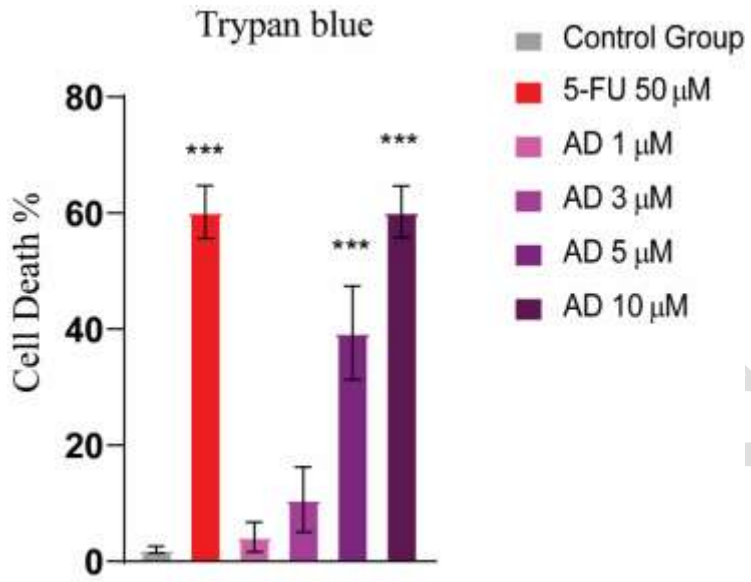

Figure 10. Trypan blue staining showed an increased cell death after treatment with Adefovir. Tukey's multiple comparison test after a one-way ANOVA, n = 3, *** ≤ 0.001.

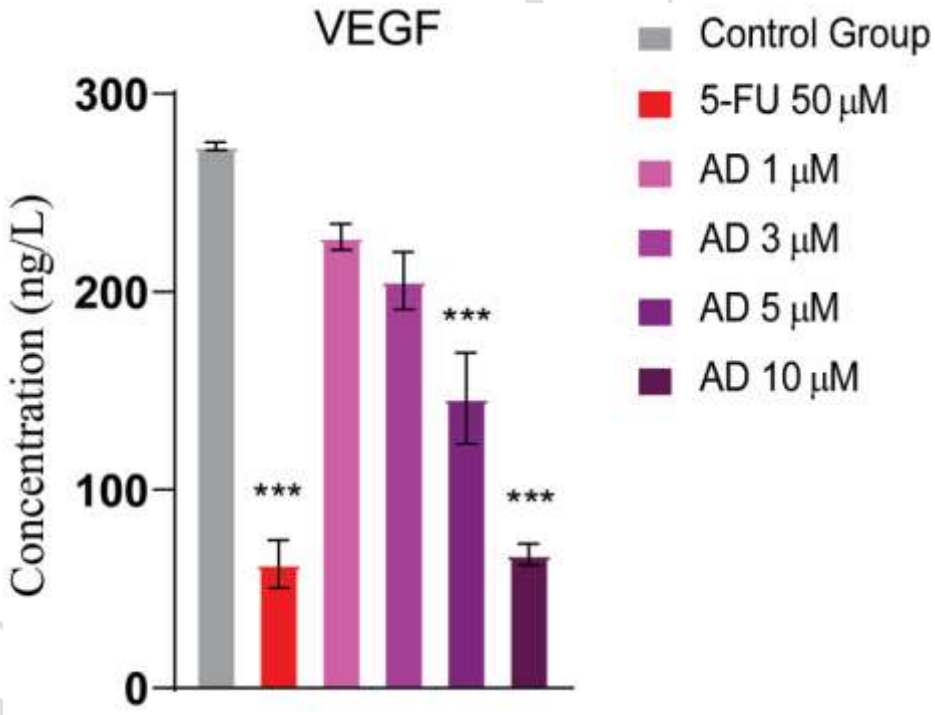

Figure 11. Vascular endothelial growth (VEGF) activity for Different Treatment Groups illustrates significant differences in treated groups as compared to the control group. Tukey's multiple comparison test after a one-way ANOVA, n = 3, *** ≤ 0.001.

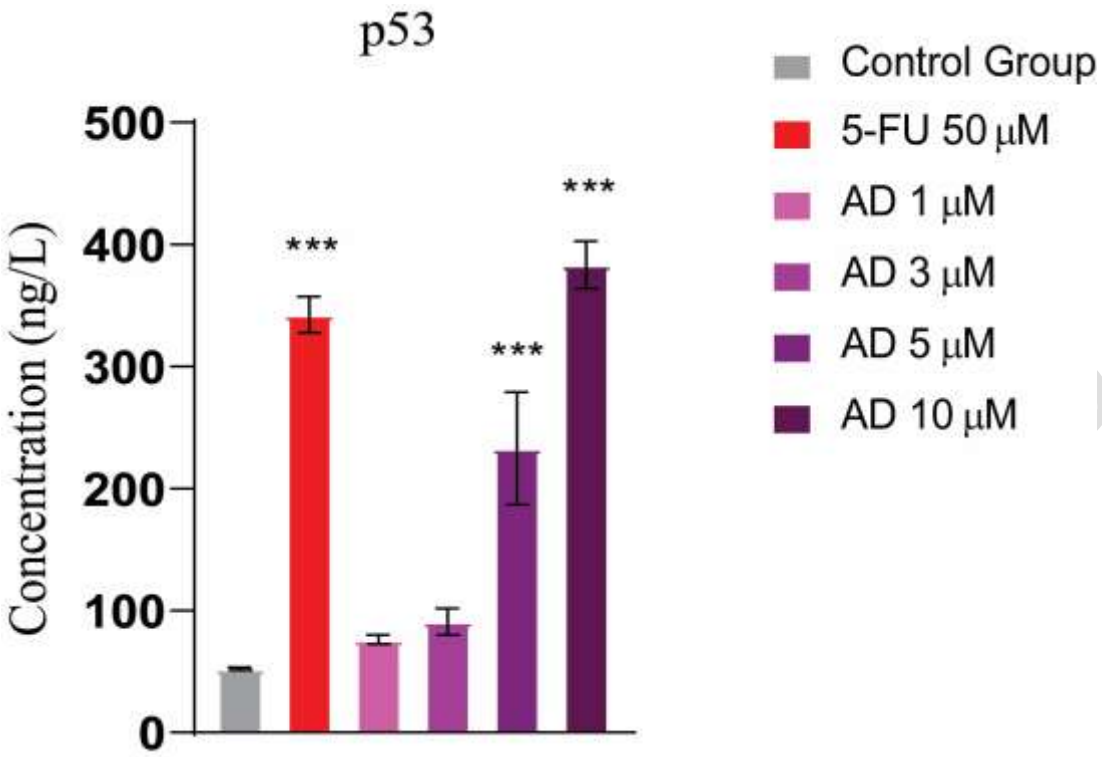

Figure 12. Expression of p53 in different treatment groups. The treated groups showed increased levels of p53 compared to the untreated control group. Tukey's multiple comparison test after a one-way ANOVA, n = 3, *** ≤ 0.001.

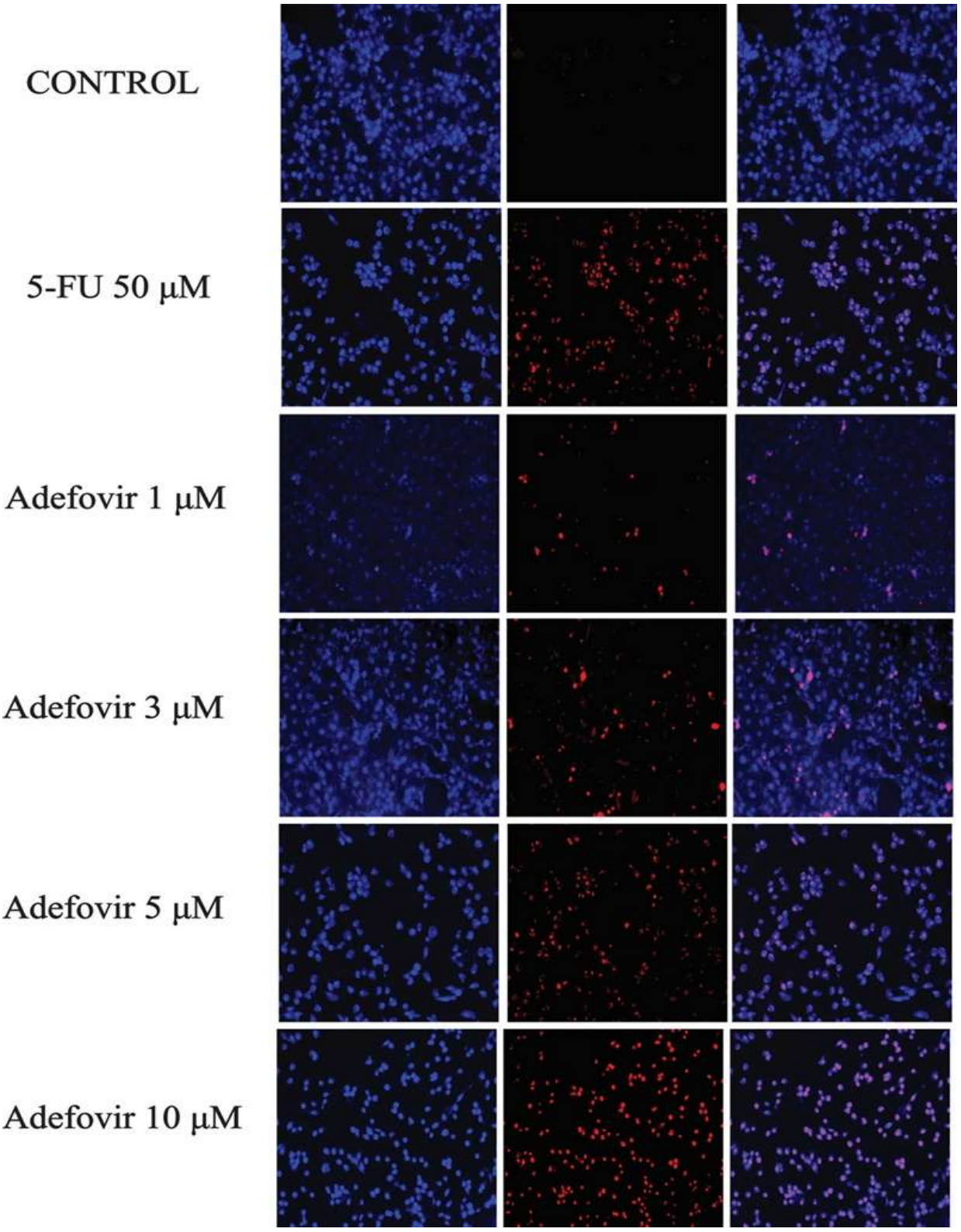

Figure 13. PI staining depicting increased cell death in adefovir and 5-FU treated groups. Blue indicates DAPI staining for nuclei, and red indicates PI staining for dead cells.